Received: 12 January 2019 | Revised: 27 June 2019 | Accepted: 28 July 2019

DOI: 10.1111/jace.16724

ORIGINAL ARTICLE

Journal of the American Ceramic Society

Measuring the effects of heat treatment on SiC/SiC ceramic matrix composites using Raman spectroscopy*

Michael W. Knauf[1] | **Craig P. Przybyla**[2] | **Andrew J. Ritchey**[3] | **Rodney W. Trice**[4] | **R. Byron Pipes**[5]

[1]School of Aeronautics and Astronautics, Purdue University, West Lafayette, Indiana

[2]Air Force Research Laboratory, Wright-Patterson Air Force Base, Ohio

[3]Rolls-Royce Corporation, Indianapolis, Indiana

[4]School of Materials Engineering, Purdue University, West Lafayette, Indiana

[5]Schools of Aeronautics and Astronautics, Materials Engineering and Chemical Engineering, Purdue University, West Lafayette, Indiana

Correspondence
Michael W. Knauf, 877 Hap Arnold Dr, Arnold AFB, TN 37388.
Email: Michael.Knauf@us.af.mil

Funding information
Research funding was provided by the US Air Force, while materials were provided by Rolls-Royce.

Abstract

The evolution of residual stresses found within a silicon carbide/silicon carbide (SiC/SiC) ceramic matrix composite through thermal treatments was investigated using Raman microspectroscopy. Constituent stress states were measured before, during, and after exposures ranging from 900 to 1300°C for varying times between 1 and 60 minutes. Silicon carbide particles in the as-received condition exhibited average hydrostatic tensile stresses of approximately 300 MPa when measured at room temperature before and after heat treatment. The room temperature Raman profile of the silicon matrix was altered in both shape and location with heat treatment cycles due to increasing activation of boron within the silicon lattice as heat treatment temperatures increased. By accounting for boron activation in the silicon–boron system, little to no permanent change of any constituent stresses were observed, and the silicon matrix subsequently exhibited a complimentary average hydrostatic compressive stress of approximately 300 MPa at room temperature, measured before and after heat treatment. This result builds upon previous literature and offers increased insight into boron activation phenomena measured through Raman spectroscopy methods.

KEYWORDS

ceramic matrix composites, Raman spectroscopy, silicon, silicon carbide, stress

1 | INTRODUCTION

Wing and Halloran[1] exploited Raman spectroscopy to report residual stress relaxation of multiple GPa in silicon melt infiltrated CMCs using high-temperature thermal treatments. Other studies have used alternative means, such as X-ray diffraction and curvature measurement, to determine residual stress relaxation in silicon at high temperatures.[2–4] The annealing time required to induce this relaxation is reported to be on the order of a few hours to a few seconds. For example, Wing and Halloran[1] annealed a similar material to the one utilized in this study at 1200°C for 5 hours, reducing the measured residual stress by nearly 50% in the silicon phase, from 2.7 GPa to 1.4 GPa; however, minimal further change in the residual stress was observed after 75 hours of additional annealing at the same temperature. Interestingly, they also note that there was no evidence of complimentary changes in the residual stress state of other CMC constituents. In contrast, other tests performed within the semiconductor industry have shown that residual stresses initially present in silicon can relax up to 90% within timeframes of seconds or less at temperatures between 900 and 1300°C, although the stress magnitudes were within a few hundred MPa instead of the GPa stresses of the previous study.[2–4]

Raman spectroscopy provides a simple and inexpensive method to determine residual stresses on a microscale

*Based upon Knauf dissertation entitled "Effects of Heat Treatment on SiC-SiC Ceramic Matrix Composites," Purdue University, 2017. Partially presented at 2018 United States Advanced Ceramics Association conference, Cape Canaveral, FL.

in silicon and silicon carbide, both common constituents in high-performance CMCs.[5,6] Employment of these methods to determine stresses in silicon, however, requires consideration of dopants (additives) found within the silicon lattice as well as known loading conditions.[7–9] Boron itself is a common dopant in silicon melt-infiltrated composites.[10] The addition of dopants, such as boron, to silicon will significantly alter the Lorentz silicon profile into an asymmetric Fano profile, changing the profile width, symmetry, and location.[11–13] Without taking these effects into account, Raman data is easily misinterpreted to conclude the silicon residual stress state is changing significantly, when in fact it is not. To gain an understanding of how dopants affect silicon and can alter Raman data, we must review the mechanisms at hand in heat treating-doped silicon.

The electrical conductivity of silicon increases dramatically as dopant (eg, boron) atoms are substituted for silicon atoms within the silicon tetrahedral lattice and subsequently establish four covalent bonds between the boron atom and four surrounding silicon atoms. For this process to occur, there must be available boron to dissolve within the lattice, heat must be applied for the diffusion process of transporting boron into a new lattice site, and there must be four silicon atoms surrounding the boron atom (this can be negated when boron clusters form, in which two boron atoms are found as neighbors and render both boron atoms electrically inactive).[14] If these requirements are met, the silicon becomes a charged, electrically active semiconductor.

The presence of electrically active boron above approximately 5×10^{18} atoms/cm^3 alters the Lorentz profile characteristics of Raman spectra collected on silicon. Above this concentration, the profile takes on an asymmetric Fano line shape.[15] This line shape is described by Equation 1 below, where ω is the abscissa, ω_0 is the Fano wavenumber, q is the asymmetry parameter, Γ is the half width at half maximum (HWHM), and I_0 is a fitting constant. Further discussion on the utilization of these parameters is found in previous work.[9]

$$I(\omega)_{\mathrm{i,Fano}} = \frac{\mathrm{I}_0 \left(q + \left(\frac{\omega - \omega_0}{\Gamma} \right) \right)^2}{1 + \left(\frac{\omega - \omega_0}{\Gamma} \right)^2} \quad (1)$$

As the amount of electrically active boron increases within the silicon lattice, the Fano profile becomes increasingly asymmetric, the width increases, and the characteristic wavenumber decreases.[11] Utilizing a least-squares fitting routine, the Fano parameters can be obtained from the Raman spectra and are readily utilized to determine the hydrostatic stress state of boron-doped silicon.[9,16] Notably, the term "hydrostatic" is used throughout this paper not to imply an isotropic stress state, but to instead refer to the mean of the normal stress components of the stress tensor. The stress states of the particles and matrix are presumed to be complex and are indeterminate without making assumptions about the loading conditions. Few, if any, loading condition assumptions could be reliably made in the various constituent cases presented; as such, the only stresses presented are simple hydrostatic stresses, readily obtained through Raman spectroscopy methods.[7,8]

The solubility of boron in silicon increases up to the eutectic temperature around 1385°C.[17] The boron solubility then decreases upon further heating, until a liquid state is reached. The maximum solubility of boron within silicon at the eutectic temperature is on the order of 1%-3%.[17,18] Given a sufficient amount of time, boron will dissolve up to the solubility limit at the respective temperature; this assumes the amount of boron atoms in the system is sufficient to achieve the solubility limit. By increasing temperature, the solubility limit increases and additional boron will dissolve into the silicon lattice. With increasingly higher annealing temperatures, additional boron can therefore dissolve and activate the silicon–boron system to higher levels.

When a material is cooled, the solubility limit decreases, and given a sufficient length of time, precipitates will form. The amount of time required for precipitation varies many orders of magnitude, from milliseconds to many years, and depends strongly on temperature.[14] Quenching the material quickly from high temperatures will prevent silicon borides from precipitating and will keep the boron in a supersaturated condition. Indeed, the semiconductor industry utilizes very fast heating and cooling rates to dissolve large amounts of boron while minimizing gross diffusion and precipitation to maximize certain desired electrical properties. Rapid thermal annealing, flash lamp annealing, and laser annealing operate on timescales of a few seconds to tens of nanoseconds with cooling rates of 1500°C/min or higher.[19,20] Conventional furnace annealing is a comparatively slow process with cooling rates on the order of 100°C/min or slower.[17] Slow cooling can cause silicon boride precipitates to remove boron from the silicon solvent if the dissolved boron concentration is over that of the solubility limit at the respective temperature. The formation of silicon boride precipitates will drive the dissolved boron to follow the solubility line down as temperature decreases, and when cooled relatively slowly, a lower amount of boron may be dissolved at room temperature compared to that found at high temperature.[19] Localized depletion of dissolved boron around these precipitates has been shown to occur, resulting in regions of low amounts of boron immediately surrounding the vicinity of the precipitate as the precipitate robs the surrounding silicon of boron.[17,21] Therefore, the activated boron levels depend on the surrounding microstructure. Subsequently, it is not unexpected that silicon in the vicinity of varying CMC constituents may exhibit varying degrees of activated boron.

Despite the previous studies, the time and temperature-dependent evolution of residual stresses within CMCs

containing silicon, and the role doped silicon plays in these changes is still not well understood, partially due to previous studies not taking activated boron within silicon matrices into account. In this study, we have investigated residual stress relaxation in a slurry melt-infiltrated ceramic matrix composite using Raman spectroscopy in both ex situ and in situ environments. The hypothesis considered here is that room-temperature constituent residual stresses will relax as both heat treatment temperatures and time at high temperatures increase. The material system considered in this work is a Rolls–Royce composite produced with Hi-Nicalon™ fibers woven into a five-harness satin weave, coated with boron nitride and silicon carbide, and subsequently infiltrated with silicon carbide particles and a boron-doped silicon matrix.

2 | EXPERIMENTAL PROCEDURE

2.1 | Sample preparation

Specific details of sample preparation and Raman spectroscopy measurements can be found in previous literature.[9] Ex situ and in situ heat treatments were both performed; ex situ testing utilized one CMC sample 25 mm × 25 mm × 4 mm in size (4 mm in the transverse direction) and one CMC sample 4 mm × 3 mm × 4 mm in size. The size differences allowed comparison between the two samples to ensure no significant stress relaxation occurred as a result of sectioning, as small samples were required for in situ measurements. In situ tests utilized a 7 mm-diameter furnace, which required samples to have maximum rectangular dimensions of 4 mm × 3 mm × 4 mm (seen in Figure 1). All measurements were taken on sample faces which were polished to a 1 μm finish; ex situ specimens were re-polished following furnace heat treatments to a 1 μm finish. Following polish, in situ samples were placed in a portable vacuum container until required for testing. Specimens were under vacuum no fewer than three weeks prior to annealing to allow trapped air to escape.

2.2 | Ex situ Raman spectroscopy measurement procedure and heat treatment

The 514.5 nm line of an Ar+ laser (Stellar-REN, Stellar Pro) was used with a Raman microscope system (Renishaw inVia, Renishaw PLC) incorporating a backscattering arrangement. A laser spot size of approximately 1 μm was produced with a 100× objective. The Raman shift of a single crystal silicon standard reference at room temperature was used to calibrate the equipment.

Multiple constituents were observed before and after heat treatment using the Raman system for ex situ measurements: silicon carbide particles (which are translucent to the 514.5 nm light[22] and allow collection of spectra from the silicon below), silicon found on the surface of the matrix, and silicon between the individual fibers within the fiber tow (ie, intratow silicon). The effective penetration depth for SiC particles using the 514.5 nm is greater than 700 μm,[9,22] much larger than the SiC particles investigated, while the effective penetration depth for silicon is approximately 0.67 μm.[9,23] This essentially returns a surface measurement for silicon interrogated on the surface of the CMC; however, the silicon stress state is much more complex and three-dimensional for silicon found underneath SiC particles. Figure 2 illustrates the overall microstructure of the investigated CMC material. No fewer than sixty point measurements were taken from each type of area, before and after heat treatments. To stay consistently away from the edges where stress gradients could be expected, spectra were obtained at random from the central specimen region, spanning no more than ~1000 μm from the center. Measurements following heat treatment occurred in the same general locations on the cut faces as the as-received measurements.

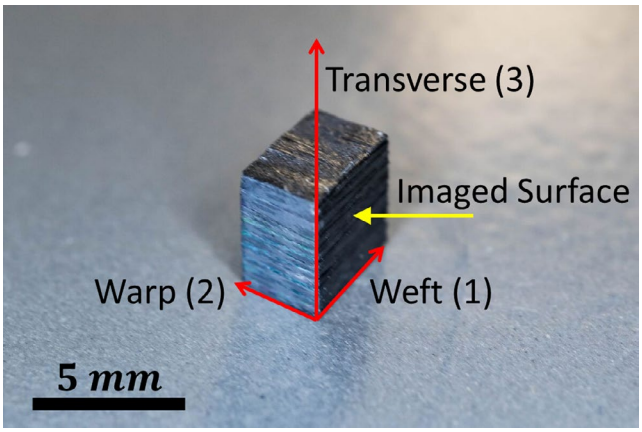

FIGURE 1 Pictured is an example of an in situ sample. Measurements were taken parallel to the warp fiber direction in the central one-half of material. Samples measured 4 mm × 3 mm × 4 mm [Color figure can be viewed at wileyonlinelibrary.com]

After pretreatment measurements were taken, specimens were heat treated in a graphite furnace at the Air Force Research Laboratory at Wright Patterson Air Force Base. The furnace chamber was initially evacuated; to ensure contaminants were not introduced at high temperature, a 99.9997%-pure argon purge was introduced at approximately 10 kPa above ambient pressure prior to heating. The furnace heated at a rate of 40°C/min to 1300°C, held 1300°C for 1 hour, and cooled at a maximum rate of 50°C/min. This cooling profile was maintained through 1100°C, at which point the set cooling rate was faster than the heat loss the furnaces could provide. Full cool down took five hours.

2.3 | In-situ Raman spectroscopy measurement procedure and heat treatment

Preliminary experiments showed that even under an initial vacuum and subsequent argon purge, small amounts of oxide

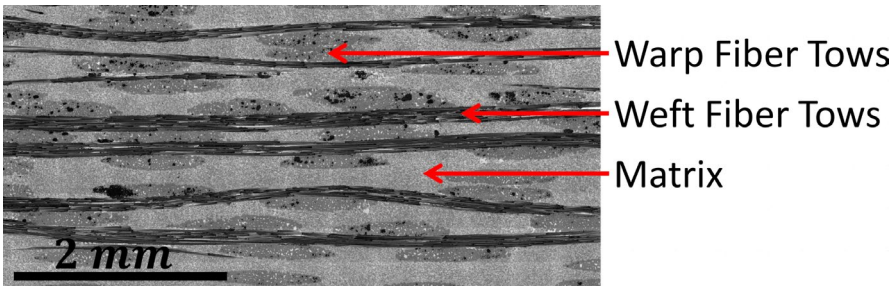

FIGURE 2 The CMC microstructure shows weft fiber tows as horizontal features, warp fiber tows as flat ellipses, and slurry melt-infiltrated matrix as the light gray speckled area. The matrix includes both silicon carbide particles and boron-doped silicon [Color figure can be viewed at wileyonlinelibrary.com]

formed on the silicon surface at temperatures above 1000°C. This was due to trapped oxygen escaping at high temperature from both voids in the CMC and the alumina furnace. The silicon beneath silicon carbide particles was therefore chosen to be examined, minimizing the effects of the oxide formation at high temperature as the silicon carbide particle protected the subsurface silicon from the thin oxidized layer. This in situ measurement was accomplished by focusing the laser on a SiC particle and observing the silicon return signature.

A Linkam heated stage (Linkam TS1500, Linkam Scientific Instruments) was utilized to heat specimens to various temperatures. The Linkam stage includes an alumina furnace, 7 mm in diameter and 6 mm in depth. The heating element is a platinum/iridium wire capable of sustaining 1500°C. A Type S thermocouple provides temperature accuracy of ±1°C. The stage can be placed under vacuum and/or introduce inert environments through various ports. A picture of this stage is shown in Figure 3 with the cover off and a CMC specimen inside the crucible. The accessory leads were not used in this experiment.

Multiple preliminary heat treatment trials were performed at high temperature to assess the influence of time and temperature on the stress state of silicon and silicon carbide particles. Specimens were randomly chosen by a computer randomization algorithm from a group of more than 50 available specimens. A vacuum was applied after loading the specimen into the Linkam stage and reattaching the sealing cover. With the vacuum applied to the stage, argon gas (99.9997% purity) was introduced at a rate of 30 cc/min for no fewer than 15 minutes prior to heating. The vacuum was turned off to perform the heat treatments in an argon environment at atmospheric pressure. All heat treatments employed heating rates of 60°C/min, with cooling rates of 100°C/min. Raman spectra were taken at room temperature before and after treatments, and at various temperatures according to the specific investigation, as outlined below.

In situ studies were performed to ascertain the time required to affect boron activation found through heat treatment. Six distinct experiments were performed on separate

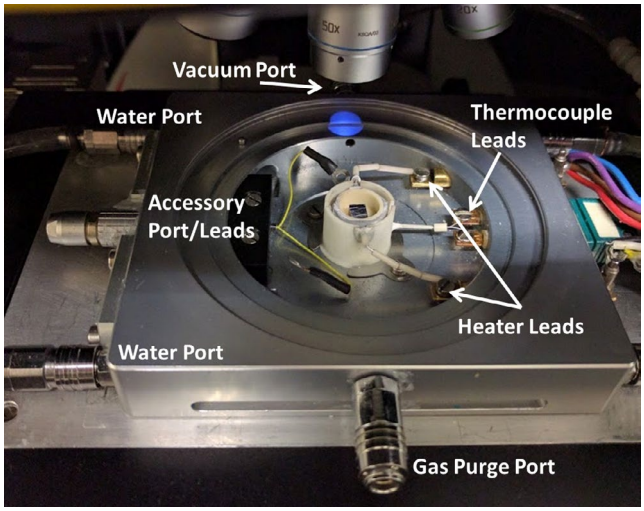

FIGURE 3 A Linkam TS1500 heated stage was utilized in the present study. Prior to heating, a ceramic radiation shield was placed on top of the crucible for thermal stability, and a water-cooled lid was then attached to allow observation through the Raman microscope [Color figure can be viewed at wileyonlinelibrary.com]

specimens and consisted of observing the Raman spectra of various SiC particles and the silicon underneath the particles before, during, and after maximum temperatures of 1000, 1050, 1100, 1150, 1200, and 1250°C, respectively. Measurements of five particles per specimen were taken at room temperature before and after heat treatment. Additional measurements were taken at 900°C, a temperature which was previously verified to cause no changes to the Raman spectra through long dwell times of at least 30 minutes. From the 900°C dwell point, temperatures were ramped to the various maximum temperatures, held at temperature for one minute (the lowest amount of time allowed by the furnace controller), and brought back to the 900°C dwell point for additional measurement. The 900°C measurement allowed for rapid verification of any changes to silicon and SiC Raman spectra due to heat treatment. This sequence was performed four times for each specimen prior to final cool down. An example microstructure is shown as a brightfield image in Figure 4, where Particles 1-5 are labeled and subsequently measured

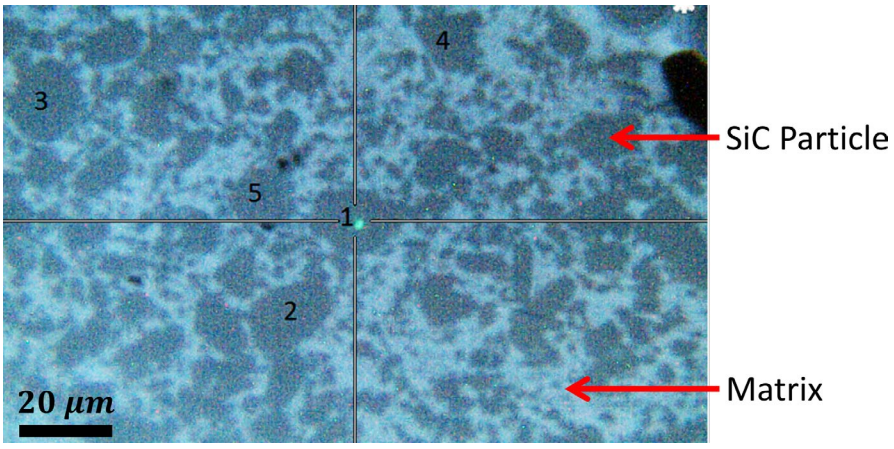

FIGURE 4 Shown is an example of a CMC matrix area where five particles were tracked through heat treatments. Dark bodies are silicon carbide particles, opaque to green laser light. The light area surrounding the silicon carbide particles is the doped-silicon matrix [Color figure can be viewed at wileyonlinelibrary.com]

during each of the four heat treatments. This methodology allowed for relatively quick documentation of fluctuating Raman spectra through heat treatment.

A final heat treatment regime included observing spectra at room temperature after each maximum temperature of 1100, 1150, 1200, 1250, and 1300°C. In this way, the room temperature hydrostatic stress of the silicon and silicon carbide could be deduced after each heat treatment for each SiC particle. Heat treatments included 5-minute holds to ensure all stress relaxation and boron activation effects were captured. Raman spectra of 15 particles were recorded before the first heat treatment and after each subsequent heat treatment. In this way, the entire temperature regime of interest was captured in a single test in which the same particles were tracked throughout the various heat treatment temperatures.

2.4 | Data reduction

MATLAB was utilized to fit the entire Raman spectrum concurrently, using Lorentzian curves for silicon carbide,[24] Lorentzian and Gaussian curves for Hi-Nicalon™ fibers,[25] and Fano curves for the primary silicon peaks.[9,11] The wavenumbers of silicon carbide were directly correlated to hydrostatic stress.[24] Silicon stresses were calculated utilizing previously reported stress conversions,[9] taking into consideration the Fano wavenumber and Fano half-width of the primary silicon peak near 520.5 cm^{-1}.

3 | RESULTS AND DISCUSSION

3.1 | Ex situ results – Silicon carbide particles

More than 60 SiC particles were analyzed before and after ex situ heat treatment at 1300°C for 1 hour. There were no indications of boron diffusion or electronic activation within SiC particles throughout heat treatments as the temperatures under investigation were considerably lower than preferred temperatures for boron diffusion in silicon carbide.[26] It should also be noted that no LO-phonon-plasmon coupling is allowed at the measured E_{2T} peak,[27] and any changes in peak position measurements can reliably be attributed to a change in stress. The average hydrostatic stress in the as-received material was found to be 270 MPa, while the average stress for the heat-treated material was 300 MPa, with standard deviations of 210 MPa and 240 MPa, respectively. The difference of 30 MPa is not statistically significant according to *t* test results of the dataset, nor was there a statistical difference between the large and small specimen sizes.

A common Raman spectrum of 6H α-SiC is shown, along with the triplet profile fit, in Figure 5. A powder of raw, unstressed SiC particles used in the manufacture of the interrogated CMC was analyzed and verified to be of the 6H SiC polytype using Raman spectroscopy.[28] No SiC spectra under investigation displayed peaks identifying any other polytype in the CMC. The main transverse optic peak (nominally at 789 cm^{-1}) is found at 787.91 cm^{-1} through the fitting routine. This corresponds to a tensile hydrostatic stress of 310 MPa.[9,24] The error due to fitting of the 787.91 cm^{-1} peak is 0.02 cm^{-1}, while the average fitting error for all 120 SiC particle 789 cm^{-1} peaks is 0.05 cm^{-1}, corresponding to 15 MPa. There is no appreciable difference between as-received and heat-treated fitting statistics. The other two peaks in Figure 5 are found at 766.81 cm^{-1} and 797.32 cm^{-1}. An additional SiC peak is found at about 974 cm^{-1}; however, this is convoluted with a broad silicon peak which does not follow a common line shape (the silicon signature is owed to the transparency of silicon carbide). Therefore, fitting of these two peaks is not performed.

3.2 | Ex situ results – Intratow silicon

Ex situ Raman spectroscopy results displaying the connection between Fano wavenumber and peak half-width of doped silicon found within the fiber tows are shown in Figure 6, utilizing previously developed methodologies.[9] The circles

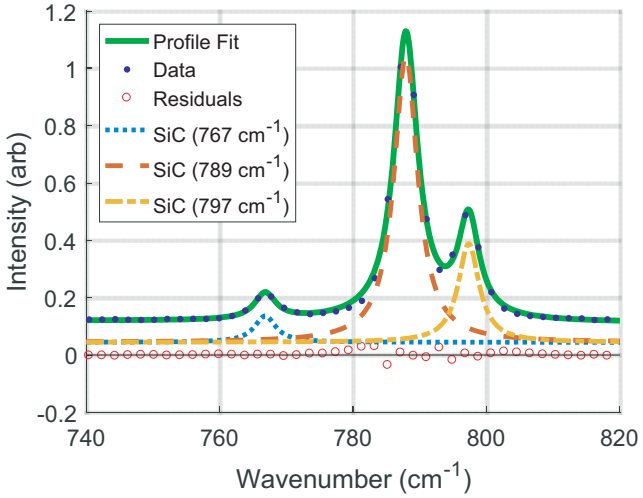

FIGURE 5 An α-SiC (6H) Raman spectrum displays three overlapping peaks which must be fit concurrently. The main central peak, at approximately 789 cm^{-1}, was utilized for residual stress measurement. The small closed circles indicate normalized data, while the various dashed lines provide the triplet curve fit. The thick solid line indicates the overall fit (including a linear baseline). Residuals are shown on the same plot along the horizontal axis as open circles [Color figure can be viewed at wileyonlinelibrary.com]

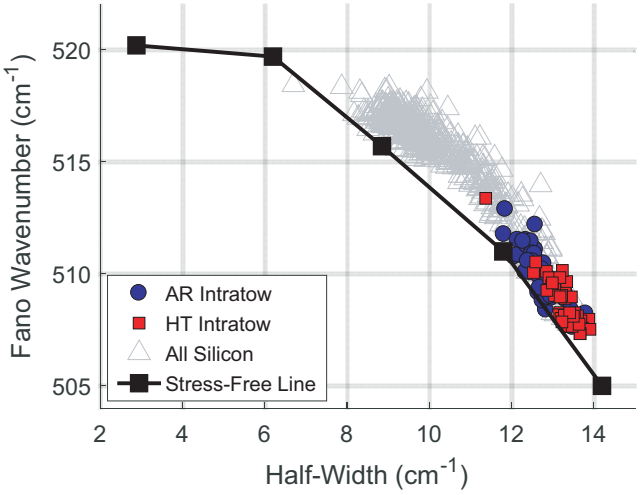

FIGURE 6 A map of the as-received and heat-treated intratow silicon values are shown, with the as-received values represented by circles and the heat-treated values represented by squares. Although the characteristic wavenumbers of the silicon did change with heat treatment, the overall stress state did not, as evidenced by the heat-treated values descending parallel to the stress-free line. The change is due to additional boron activation within the silicon lattice. Subdued triangles provide reference to all other silicon measurements taken during testing [Color figure can be viewed at wileyonlinelibrary.com]

display the as-received silicon values, while the squares indicate heat-treated values. Subdued triangles are shown of all collected silicon data from previous studies for comparison.[9] Juxtaposed to the as-received values, significant changes occurred in the Raman profiles of the intratow areas due to heat treatment of 1300°C for one hour. The mean Fano wavenumber decreased from 510.01 cm^{-1} to 508.96 cm^{-1}, and the mean asymmetry parameter decreased from 2.44 to 2.21. Finally, the mean half-width increased from 12.72 cm^{-1} to 13.27 cm^{-1}. All three of these indicate that the heat treatment activated additional boron found within the composite. However, these wavenumber changes do not necessarily indicate that the stress state changed. Without taking the expanded Chandrasekhar[9,11] stress-free conditions into account, the change in wavenumbers would have resulted in an incorrect calculation, assessing a tensile change in stress of 230 MPa. Utilizing the stress-free line, a statistically insignificant change of compressive stress of approximately 10 MPa was recorded, where the as-received hydrostatic stress is −240 MPa and the heat-treated hydrostatic stress is −250 MPa.

3.3 | Ex situ results – Surface silicon

The silicon found on the surface of the matrix exhibited the largest gradients of activated boron within the material, as seen by the large range in both wavenumber and half-width values in Figure 7. The as-received wavenumbers ranged from 510 cm^{-1} to 517 cm^{-1} (mean of 513.65 cm^{-1}), and the heat-treated wavenumbers ranged from 508 cm^{-1} to 515 cm^{-1} (mean of 510.95 cm^{-1}). The half-widths followed the wavenumbers along the trendline; however, the stress ranges are considerably less than would have been otherwise found if the trendline were not used to determine stress state. The mean half-width increased with heat treatment from 11.18 cm^{-1} to 12.56 cm^{-1}, while the asymmetry parameter decreased from 3.13 to 2.56. The mean standard error due to fitting was 0.11 cm^{-1}, corresponding to approximately 20 MPa, with no appreciable difference between the as-received and heat-treated standard errors. Finally, the as-received stress state decreased from −320 MPa in the as-received condition to −340 MPa after heat treatment.

3.4 | Ex situ heat treatment discussion

Given a constant measurement temperature, a decrease in wavenumber from a stress-free state in any material is generally indicative of an increase in tensile stress. Lengsfeld et al[29] noted boron-doped silicon exhibited a decrease in wavenumber which was not observed in silicon free of dopant; they suggest this wavenumber shift may be due instead to an increase in the tensile stress found between the bonded boron and silicon atoms within the silicon lattice. Boron has a smaller atomic radius than that of silicon,[30] which could explain this wavenumber shift as the smaller radius would create tension on the atomic bonds between boron atoms and the surrounding silicon. However, the lack of a complementary large shift in SiC particle stresses indicates that if this is a correct assessment, the stresses are not changing even on a

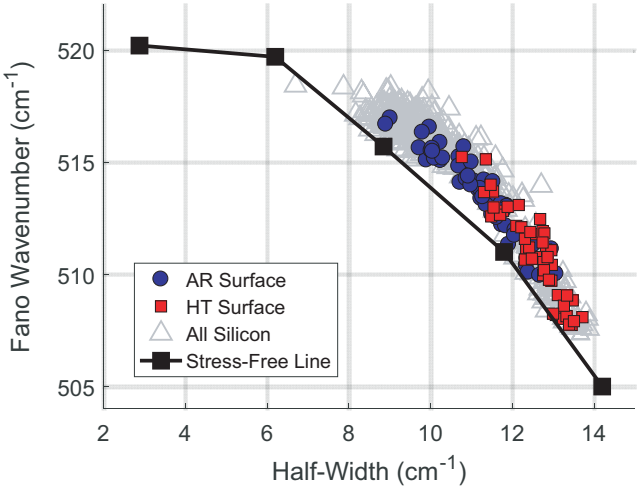

FIGURE 7 A map of the as-received and heat-treated silicon Raman values found on the matrix surface are shown, with the as-received values as circles and the heat-treated values as squares. The variance found in these areas indicates large gradients of activated boron within the general silicon matrix. Subdued triangles provide reference to all other silicon measurements taken during testing [Color figure can be viewed at wileyonlinelibrary.com]

microscale. Instead, this explanation limits the stress change to only the atomic lattice scale, as these stresses would self-equilibrate within the local region around the boron atoms.

Phonon confinement effects were also considered as a potential source of variability through heat treatments. Although the phonon confinement effect can generate an asymmetric Raman profile, the phonon confinement model does not account for the characteristic anti-resonnance dip found in the Fano profile[31] on the lower-energy side of the curve (eg, for boron-doped silicon). All silicon profiles investigated in this work included this anti-resonance, providing confidence that Fano interference/boron activation is occuring. Additionally, where Sagar et al[31] observed increasing asymmetry with increasing excitation energy for a given nanocrystal size, we observed the opposite to be true, where asymmetry increased substantially when the silicon phase was interrogated with a lower-energy 633 nm laser (vs the 514 nm laser used for the majority of experiments). This behavior is indicative of Fano intereference affecting the Raman lineshape, rendering phonon confinement effects to be of minimal impact. Finally, more than 500 silicon crystallites were analyzed through the use of transmission XRD to observe changes in coherent domain size before and after similar 1300°C heat treatments to those described above. The coherent domain size was estimated for each crystallite using the Scherrer equation for spherical particles of a cubic lattice, and were judged to stay constant (within 1 nm) before and after heat treatments of 1250°C for times between 5 and 30 minutes at temperature. If the phonon confinement effect were active and contributing to fluctuations in the Raman profile, we would expect to see changes in the XRD results under similar conditions.[32] In light of these results, we propose the contributions in variability are due solely to boron activation within the silicon lattice and phonon confinement effects do not require consideration.[33–35]

A summary of the effects of heat treatment on various constituents is presented in Table 1. Overall the SiC particles are found to be in a state of residual tension, while the silicon is found to be in a state of residual compression. As shown previously in Figure 4, the microstructure of melt infiltrated SiC/SiC CMCs is highly variable at the ~1 μm scale sampled by the Raman laser. To capture the average stress state in the various phases, a significant number of measurements were taken throughout the samples. As expected, the measurements taken on a specific phase had a large amount of variation, which contributes to expected large standard deviations; the average of these stresses converge to the true mean of the constituent with sufficient data points, per the central limit theorem.[36,37] In all cases, the current measurements showed that the change in the phase averaged residual stress (on the order of tens of MPa) as a result of heat treatments was insignificant relative to the baseline variation. This conclusion was confirmed through the full statistical analysis, as well as through measurements repeated on the sample loci through the heat treatment cycles. This conclusion is a significant contribution considering previous literature which reported substantial changes (on the order of one GPa) to the state of residual stress in similar materials.[1] The final column contains *t* test *P* values, where the null hypothesis claims there is no change to the stress state due to heat treatment (the calculated *P*-values fail to reject this claim).

The major change observed with this heat treatment stems from the high amounts of activated boron within the silicon matrix. This electrical activation with heat treatment is a common trait throughout melt-infiltrated CMCs, as Gordon[38]

TABLE 1 Summary of effects of heat treatment on various as-received (AR) and heat-treated (HT) constituent wavenumbers (ω_0), hydrostatic residual stresses (σ_H), and stress standard deviations (s_H)

Constituent	AR Mean ω_0 (cm^{-1})	HT Mean ω_0 (cm^{-1})	AR Mean σ_H (MPa)	HT Mean σ_H (MPa)	AR Std Dev s_H (MPa)	HT Std Dev s_H (MPa)	*P*-value
SiC particles	788.05	787.94	270	300	210	240	.48
Intratow silicon	510.00	508.69	−240	−250	110	100	.63
Surface silicon	513.65	510.95	−320	−340	100	140	.33

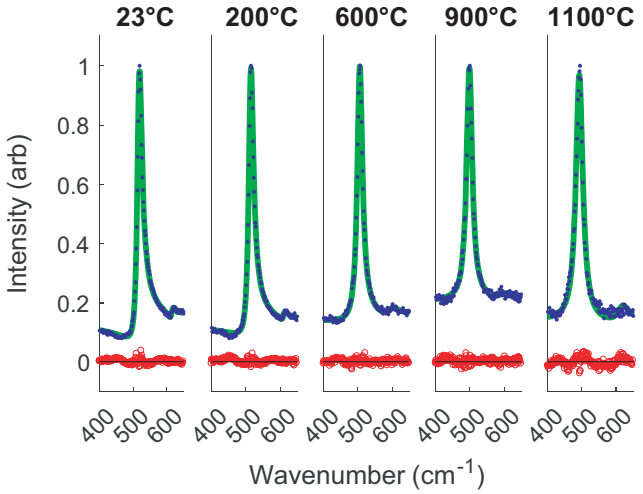

FIGURE 8 The doped silicon Fano asymmetry reduces with increasing temperature. The closed circles show normalized data while the thick superimposed line is the curve fit. Residuals are shown as open circles along the horizontal axis. Silicon Raman spectra were taken at (left to right) 23, 200, 600, 900, and 1100°C. Raman acquisitions were taken from the identical SiC particle location for all measurements. Heating doped silicon above room temperature transitions the Fermi level out of the valence band into the band gap and is manifested as reduced Fano profile asymmetry (increased Fano asymmetry parameter) as temperature increases [Color figure can be viewed at wileyonlinelibrary.com]

noted thermal treatments produced a highly conductive matrix in a similar melt infiltrated CMC material. Additionally, the shifts observed in wavenumber with heat treatment are very similar to those described by Wing and Halloran[1] with comparable heat treatments. Without accounting for boron activation, very large changes in the silicon stress state could otherwise be recorded for CMCs containing significant boron dopant due to heat treatment in this temperature regime.

3.5 | In situ results – Raman profile at high temperature

The Fano profile found in the doped silicon became more symmetric when measured in situ at high temperatures. Increasing temperatures affect the electrical properties of the doped silicon matrix as this serves to drive the Fermi level out of the valence band and into the band gap.[39] Because Fano resonance is a product of the Fermi level entering the valence band, increasing temperatures serve to decrease and may remove the Fano resonance altogether, depending on the dopant level and temperature attained.[9] This effect is seen in Figure 8. At 23°C (far left curve in Figure 8), the asymmetry is unmistakable, and includes an additional Fano profile at 620 cm^{-1} due to the boron dopant[9]. Through 200°C and 600°C, the asymmetry continues to recede, while at 900 and 1100°C the profile becomes a near-perfect Lorentzian curve (as $q \to \infty$, the Fano profile limits to a Lorentzian profile). The additional scatter observed in the 1100°C profile is caused by the increasing amounts of black body radiation emitted at these temperatures; this radiation is indistinguishable from light produced through the Raman effect. Planck's Law is utilized in conjunction with a linear baseline to separate the background intensity from the detected Raman profile at temperatures above 900°C. Even with this adjustment, without significant measurement times, the resulting profile at 1100°C is inferior to other profiles at cooler temperatures due to the considerable background light emitted from the specimen. The Fano profile returns (and is more asymmetric due to increased boron activation) after the material cools back to room temperature. The asymmetry values changed minimally as 1100°C (the maximum temperature attained for this particular sample) appears to be close to a lower limit for boron activation in this CMC. Values for the profiles are provided in Table 2.

3.6 | In situ results – Effects on subsurface silicon

In situ experiments which tracked five particles through minute-long heat treatments at consistent temperatures displayed no significant changes in any Fano parameters (wavenumbers, half-widths, or asymmetry parameters) in samples heat treated at temperatures less than 1100°C. At temperatures greater than or equal to 1100°C, the primary changes to the Raman spectra occurred within the first minute of heat treatment. Subsequent time at temperature had little to no effect on the Fano profile (i.e., activated boron concentration). This is consistent with boron activation times occurring on the order of seconds or less, as discussed above. Silicon Fano wavenumbers decreased as much 1.5 cm^{-1} with a 1250°C heat treatment in the first minute, though neither silicon nor silicon carbide stresses changed significantly through heat treatment and stress magnitudes were consistent with results above.

The in-situ experiment which tracked 15 particles through an increasing heat treatment process indicated significant decreases in the Fano wavenumber of subsurface silicon after each heat treatment, as shown in Figure 9. This specific specimen underwent five-minute heat treatments at the displayed temperatures and the specimen was brought back to room temperature each time for measurement. The data taken from these 15 points are shown by the various solid shapes, while the Chandrasekhar stress-free line is shown as the solid line, and the data are set against a backdrop of subdued open triangles, representative of all silicon measurements made in the study. The trend is clearly defined as the Fano parameters decrease parallel to the stress-free line developed by Chandrasekhar[11] and previous work,[9] indicating the amount of activated boron is increasing within the silicon grains. This is consistent with the findings of earlier sections. Estimating activated boron concentrations was not

TABLE 2 Fano wavenumber and asymmetry of silicon found beneath common SiC particle at various temperatures, while heating (H) and cooling (C)

Temperature	23°C	200°C	600°C	900°C	1100°C	900°C	600°C	200°C	23°C
Heating/Cooling	H	H	H	H	H	C	C	C	C
Fano ω_0	516.72	513.58	505.24	498.56	492.60	498.35	504.97	513.21	516.24
Asymmetry parameter	3.9	5.2	15.0	270	∞	260	14.2	5.1	3.8

specifically attempted; however, additional refinement and calibration of the utilized techniques would allow for reliable estimation of activated boron within silicon. This could be especially advantageous as dopant concentration can affect mechanical properties[40].

As shown in Figure 10, there was very little change in the hydrostatic stress state of doped silicon due to these heat treatments. The average compressive hydrostatic stress stayed approximately constant within 350 MPa~380 MPa. An Analysis of Variance (ANOVA) was performed to determine if any of the heat treatments resulted in changes in the stress state of silicon after taking the Fano resonance into account. The ANOVA calculated a P-value of $P = .80$, and thus the null hypothesis that heat treatments up to 1300°C for five minutes do not affect the hydrostatic stress state cannot be rejected. If there is indeed an effect of heat treatment on the residual stress state of silicon within this material, it is likely minimal.

Silicon carbide particles were interrogated to collect silicon signals utilized in the above analyses. This allowed the silicon carbide particle signatures to be recorded concurrent to the silicon through increasing heat treatment temperatures. These stresses, determined at room temperature after the indicated heat treatments, can be seen in Figure 11. As before, the changes in stress were minimal, fluctuating a maximum of 50 MPa between the extremes. An ANOVA was accomplished on these data, resulting in a P-value of $P = .94$. Again, this demonstrates that the null hypothesis cannot be rejected, and if there are changes in the residual stress state within the silicon carbide, the changes are minimal.

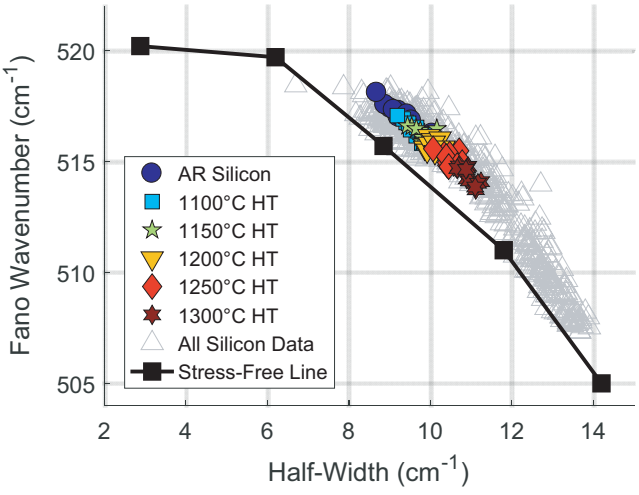

FIGURE 9 Clear evidence of increasing boron activation with increasing anneal temperature is shown above. The as-received (AR) silicon exhibits relatively low amounts of activated boron evidenced by the circles at relatively high wavenumber and low half-width values. As annealing temperatures increased, the room-temperature measurements paralleled the Chandrasekhar stress-free line, culminating in much higher levels of activated boron at the test termination as shown by the stars. Subdued triangles provide reference to all other silicon measurements taken during testing [Color figure can be viewed at wileyonlinelibrary.com]

3.7 | In situ heat treatment discussion

Boron activation in the semiconductor industry is often accomplished through heat treatments; generally, the material is cooled very quickly to lock in the desired amount of activated boron into the substitutional sites within the silicon lattice. The quenches the semiconductor industry utilize require cooling rates orders of magnitude higher than those utilized in the present experiments. Because the CMC was produced at a temperature higher than the studied heat treatment temperatures, it is interesting that the substitutional boron level is affected by heat treatments at an intermediate temperature. Multiple plausible explanations exist, as boron activation is still an active area of research. Diffusion through the lattice at high temperatures is very fast and can transport boron over relatively long distances. Because the additional boron activation occurred throughout all areas, a boron source is required. This can be in the form of boron already in substitutional positions, but inactive due to being alongside additional boron atoms. High temperatures can free these clusters and transport the boron atoms to additional substitutional sites, thus activating the boron. An alternative explanation is that present silicon borides can dissolve at high temperatures, releasing boron into the silicon lattice and increasing the activation through boride annihilation. Additionally, various elements and compounds present during manufacturing can also have an effect on the amount of activated boron. The conclusion as to the true mechanism behind the additional boron activation is uncertain, although the influence is clearly characterized through Raman spectroscopy.

The results of the in situ testing demonstrate that there are no statistically significant changes to the residual stress state as

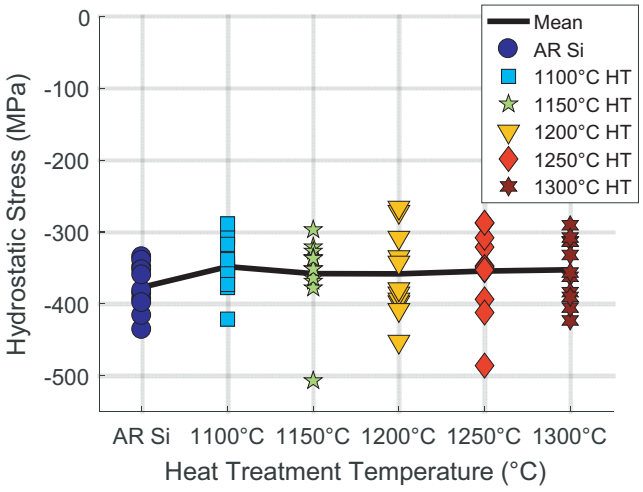

FIGURE 10 The residual silicon hydrostatic stresses are shown by increasing heat treatment temperature. All measurements were taken at room temperature. Although the wavenumbers shifted considerably, the mean stresses did not change significantly, as evidenced by the heavy mean line staying relatively constant near −350 MPa [Color figure can be viewed at wileyonlinelibrary.com]

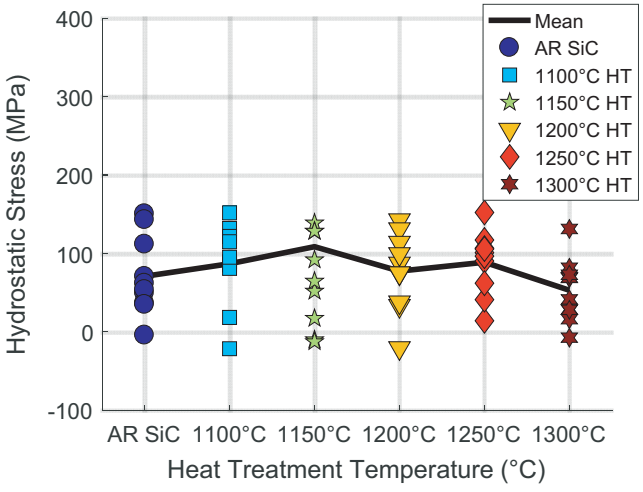

FIGURE 11 The hydrostatic stress of the corresponding silicon carbide particles to the matrix silicon are shown above. Increasing heat treatments had relatively minor impacts to the SiC stress state, with maximum fluctuations of less than 50 MPa. All measurements were taken at room temperature [Color figure can be viewed at wileyonlinelibrary.com]

a result of heat treatments for this material. If the Fano characteristics are not fully considered when boron is present, an incorrect conclusion for the stress state of the material would be assumed. The results of the in situ tests coincide with the results of previous ex-situ tests in this work and offer additional insight into the speed at which the boron activation takes place.

The conclusions drawn from the Raman spectroscopy measurements have been further confirmed through micro-XRD experiments at Argonne National Lab's Advanced Photon Source. Within this research, SiC particle average normal stresses were 290–310 MPa (tensile), depending on orientation, while silicon average normal stresses were 280–300 MPa (compressive), again depending on orientation[41].

4 | CONCLUSIONS

Stresses were found to be tensile in nature in the silicon carbide particles embedded within the matrix. The average silicon carbide particle tensile stress was found to be approximately 270 MPa in the as-received material, and 300 MPa in the same material after heat treatment at 1300°C for 1 hour. These average stresses are not statistically different. The silicon compressive stress state was shown to be relatively constant through heat treatment in all investigated areas. Hydrostatic compressive stresses between 250 MPa and 400 MPa were determined for the various areas in which silicon was found: in-between fibers, on the surface of the matrix, and underneath silicon carbide particles.

The Fano profile was found to resolve into a Lorentzian profile with increasing temperature. This is attributable to the Fermi level moving from the valence band into the conduction band with increasing temperatures. This result can possibly be utilized to determine stresses in silicon at high temperature while neglecting the effects of the boron concentration; considerable research would need to be conducted to determine if this is a viable technique.

A heat treatment of 1300°C for 1 hour concluded that considerable boron activation occurred in the silicon due to heat treatment. In situ results of heat-treated CMC specimens displayed continuously increasing amounts of boron activation with increasing heat treatment temperatures. Temperatures as low as 1100°C exhibited this increase, and the effect increased with increasing temperatures, up through at least 1300°C (the maximum studied temperature). Without taking the wavenumber decrease associated with the Fano profile/boron activation into account, major errors can be generated which can lead to significant departures from the true residual stress state.

ORCID

Michael W. Knauf https://orcid.org/0000-0003-1418-5651

REFERENCES

1. Wing B, Halloran J. Relaxation of residual microstress in reaction bonded silicon carbide. Ceram Int. 2018;44(10):11745–50.
2. Zhang X, Zhang T, Wong M, Zohar Y. Effects of high-temperature rapid thermal annealing on the residual stress of LPCVD-polysilicon thin films. Tenth Annual Workshop on Micro Electro Mechanical Systems, IEEE; 1997 Jan 26–30; Nagoya, Japan. IEEE; 1997:535–40.

3. Kotake H, Takasu S. The effect of annealing on residual stress and dislocation propagation in silicon slices with damaged layer induced by scribing. J Mater Sci. 1981;16(3):767–74.
4. Maier-Schneider D, Maibach J, Obermeier E, Schneider D. Variations in Young's modulus and intrinsic stress of LPCVD-polysilicon due to high-temperature annealing. J Micromech Microeng. 1995;5(2):121–4.
5. De Wolf I. Micro-Raman spectroscopy to study local mechanical stress in silicon integrated circuits. Semicond Sci Technol. 1996;11:139–54.
6. De Wolf I, Maes H, Jones S. Stress measurements in silicon devices through Raman spectroscopy: bridging the gap between theory and experiment. J Appl Phys. 1996;79(9):7148–56.
7. Anastassakis E. Strain characterization of polycrystalline diamond and silicon systems. J Appl Phys. 1999;86(1):249–58.
8. Anastassakis E, Cantarero A, Cardona M. Piezo-Raman measurements and anharmonic parameters in silicon and diamond. Phys Rev B: Condens Matter Mater Phys. 1990;41(11):7529–35.
9. Knauf M, Przybyla C, Ritchey A, Trice R, Pipes RB. Residual stress determination of silicon containing boron in CMCs. J Am Ceram Soc. 2019;102:2820–9.
10. Suyama S, Kameda T, Itoh Y. Effect of structure of interfacial coating layer on mechanical properties of continuous fiber reinforced reaction sintered silicon carbide matrix composite. J Mater Sci. 2002;37(6):1101–6.
11. Chandrasekhar M, Chandrasekhar H, Grimsditch M, Cardona M. Study of the localized vibrations of boron in heavily doped Si. Phys Rev B. 1980;22(10):4825–33.
12. Nickel N, Lengsfeld P, Sieber I. Raman spectroscopy of heavily doped polycrystalline silicon thin films. Phys Rev B. 2000;61(23):15558–61.
13. Cerdeira F, Cardona M. Effect of carrier concentration on the Raman frequencies of Si and Ge. Phys Rev B. 1972;5(4):1440–54.
14. Cerofolini G, Meda L. Physical chemistry of, in and on silicon. Berlin, Heidelberg, New York, London, Paris, Tokyo: Springer Science & Business Media; 2012.
15. Fano U. Effects of configuration interaction on intensities and phase shifts. Phys Rev. 1961;124(6):1866–78.
16. Agaiby R, Becker M, Thapa S, Urmoneit U, Berger A, Gawlik A, et al. Stress and doping uniformity of laser crystallized amorphous silicon in thin film silicon solar cells. J Appl Phys. 2010;107(5):054312.
17. Olesinski R, Abbaschian G. The B-Si (Boron-Silicon) system. J Phase Equilib. 1984;5(5):478–84.
18. Armigliato A, Nobili D, Ostoja P, Servidori M, Solmi S. Solubility and precipitation of boron in silicon and supersaturation resulting by thermal predeposition. In: Huff H, Sirtl E, editors. Semiconductor silicon. Princeton: Electrochemical Society; 1977: p. 638–47.
19. Lanzerath F, Buca D, Trinkaus H, Goryll M, Mantl S, Knoch J, et al. Boron activation and diffusion in silicon and strained silicon-on-insulator by rapid thermal and flash lamp annealings. J Appl Phys. 2008;104(4):044908.
20. Takamura Y, Jain S, Griffin P, Plummer J. Thermal stability of dopants in laser annealed silicon. J Appl Phys. 2002;92(1):230–4.
21. Aselage T. The coexistence of silicon borides with boron-saturated silicon: metastability of SiB3. J. Mater. Res. 1998;13(7):1786–94.
22. Derst G, Wilbertz C, Bhatia K, Krätschmer W, Kalbitzer S. Optical properties of SiC for crystalline/amorphous pattern fabrication. Appl Phys Lett. 1989;54(18):1722–4.
23. Aspnes D, Studna A. Dielectric functions and optical parameters of Si, Ge, GaP, GaAs, GaSb, InP, InAs, and InSb from 1.5 to 6.0 eV. Phys Rev B: Condens Matter. 1983;27(2):985–1009.
24. DiGregorio J, Furtak T. Analysis of residual stress in 6H-SiC particles within Al2O3/SiC composites through Raman spectroscopy. J Am Ceram Soc. 1992;75(7):1854–7.
25. Gouadec G, Colomban P, Bansal NP. Raman study of Hi-Nicalon fiber reinforced celsian composites: II, residual stress in fibers. J Am Ceram Soc. 2001;84(5):1136–42.
26. Gao Y, Soloviev S, Sudarshan T. Investigation of boron diffusion in 6H-SiC. Appl Phys Lett. 2003;83(5):905–7.
27. Harima H, Nakashima S, Uemura T. Raman scattering from anisotropic LO-phonon-plasmon-coupled mode in n-type 4H- and 6H-SiC. J Appl Phys. 1995;78(3):1996–2005.
28. Nakashima S, Harima H. Raman investigation of SiC polytypes. Phys Status Solidi A. 1997;162:39–64.
29. Lengsfeld P, Nickel N, Genzel C, Fuhs W. Stress in undoped and doped laser crystallized poly-Si. J Appl Phys. 2002;91(11):9128–35.
30. Okada Y. Diamond cubic Si: structure, lattice parameter, and density. In: Hull R, editor. Properties of crystalline silicon. London: INSPEC, 1999;20:91–7.
31. Sagar DM, Atkin JM, Palomaki P, Neale NR, Blackburn JL, Johnson JC, et al. Quantum confined electron−phonon interaction in silicon nanocrystals. Nano Lett. 2015;15:1511–6.
32. Dey S, Chatterjee P, Gupta S. Dislocation induced line-broadening in cold-worked Pb-Bi binary alloy system in the a-phase using X-ray powder profile analysis. Acta Mater. 2003;51:4669–77.
33. Richter H, Wang Z, Ley L. The one phonon Raman spectrum in microcrystalline silicon. Solid State Commun. 1981;39:625–9.
34. Rohmfeld S, Hundhausen M, Ley L. Raman scattering in polycrystalline 3C-SiC: influence of stacking faults. Phys Rev B. 1998;58(15):9858–62.
35. Meier C, Lüttjohann S, Kravets V, Nienhaus H, Lorke A, Wiggers H. Raman properties of silicon nanoparticles. Phys E (Amst, Neth). 2006;32:155–8.
36. Withers P, Bhadeshia H. Residual stress, part 1 - measurement techniques. Mater Sci Technol. 2001;17:355–64.
37. Montgomery D. Design and analysis of experiments, 6th edn. New York, NY: John Wiley & Sons; 2004.
38. Gordon N. Material health monitoring of SiC/SiC laminated ceramic matrix composites with acoustic emission and electrical resistance [master's thesis]. Akron, OH: The University of Akron; 2014.
39. Thurmond C. The standard thermodynamic functions for the formation of electrons and holes in Ge, Si, GaAs, and GaP. J Electrochem Soc. 1975;122(8):1133–41.
40. Bhushan B, Li X. Micromechanical and tribological characterization of doped single-crystal silicon and polysilicon films for microelectromechanical systems devices. J Mater Res. 1997;12(1):54–63.
41. Knauf M. Effects of heat treatment on SiC-SiC ceramic matrix composites [dissertation]. West Lafayette, IN: Purdue University; 2017.

How to cite this article: Knauf MW, Przybyla CP, Ritchey AJ, Trice RW, Pipes RB. Measuring the effects of heat treatment on SiC/SiC ceramic matrix composites using Raman spectroscopy. *J Am Ceram Soc*. 2020;103:1293–1303. https://doi.org/10.1111/jace.16724